Desalination and Water Treatment
www.deswater.com

1944-3994/1944-3986 © 2012 Desalination Publications. All rights reserved
doi: 10/5004/dwt.2012.2735

Taylor & Francis
Taylor & Francis Group

40 (2012) 100–117
February

Sensitivity of SDI for experimental errors

Abdulsalam Alhadidi[a], Bastiaan Blankert[b], Antoine J.B. Kemperman[a,*], Jan C. Schippers[c], Matthias Wessling[a], Walter G.J. van der Meer[a]

[a]*Membrane Technology Group, MESA+ Institute for Nanotechnology, Faculty of Science and Technology, University of Twente, 7500 AE Enschede, The Netherlands*
Tel. +31 53 4892956; Fax: +31 53 4894611; email: a.j.b.kemperman@utwente.nl
[b]*Pentair X-Flow, 7500 AS Enschede, The Netherlands*
[c]*UNESCO-IHE Delft, Westvest 7, 2601 DA Delft, The Netherlands*

Received 16 February 2011; Accepted 2 November 2011

ABSTRACT

Silt density index (SDI) testing is a widely-accepted method for estimating the rate at which colloidal and particle fouling will occur in water purification systems when using reverse osmosis (RO) or nanofiltration (NF) membranes. However, the SDI has several deficiencies. For example, the SDI has no linear relationship with the particle concentration, is not based on any fouling mechanism, and is not corrected for temperature, pressure and membrane resistance. The accuracy and reproducibility of the SDI is often questioned. In this study, mathematical models were developed to investigate the sensitivity of SDI for the following types of errors: errors due to inaccurate lab or field equipment, systematic errors, and errors resulting from artifacts and personal observations and experience. The mathematical results were verified experimentally. Both the mathematical models and experimental results show that the membrane resistance R_M has the highest impact on the SDI results. The allowable ASTM variation in R_M is responsible for a deviation in SDI between 2.29 and 3.98 at a level of SDI = 3. Besides that, a 1 s error in measuring the time to collect the second sample t_2 results in ±0.07 at SDI_O = 3. The artifacts and personal experience also influence the SDI results. The total error in measuring SDI was estimated to be equal to ±2.11 in the field and only ±0.4 in the lab in level of SDI_O = 3. Furthermore, several recommendations are mentioned based on these theoretical results and our personal experience. This study demonstrates the sensitivity of the SDI for errors in R_M and the accuracy of the equipments, and explains the difficulties in reproducing SDI results for the same water.

Keywords: Silt density index; Error; Testing conditions; Mathematical models; Desalination, Fouling

1. Introduction

Reverse osmosis (RO) and nanofiltration (NF) membrane systems are widely used in the desalination of water. Membrane fouling is the decline in the membrane performance with time. This results in reduced permeability, reduced retention and increased pressure drop over the spacers. The fouling can be categorized as: biofouling, scaling and particulate fouling. To evaluate and monitor the performance of the pre-treatment, a reliable index is necessary to predict the fouling potential of the RO feed water.

Estimates of the colloidal fouling tendency can be obtained by performing a fouling test such as SDI

*Corresponding author.

or MFI. The SDI test can be used to compare different pretreatment methods [1,2], design new desalination plants [3,4] and monitor performance of the treatment [5]. The ASTM describes the SDI test as a standard test for particulate RO fouling potential. The SDI test is applied already for decades worldwide [6]. The SDI test compares the initial flow rate to the flow rate after 15 min filtration using microfiltration (MF) membranes with an average pore size of 0.45 µm. MF membrane properties such as pore size, porosity, hydrophilicity, zeta potential, and surface roughness affect the fouling rate during the SDI test [7–15]. Furthermore, colloid nature and water properties affect the MF fouling rate [7,16–18].

Recently, there are growing doubts about the predictive value of SDI. In addition there are several deficiencies observed, which affect the accuracy and reproducibility, for example [15,16,18,19]:

- No correction factor for temperature;
- No correction for variations in membrane properties;
- No linear correlation with the concentration of colloidal/suspended particles.

In this work, the sensitivity of SDI for errors due to low accuracy of the testing equipment, variable membrane properties, and variation in the testing parameters was studied theoretically and experimentally. In addition, specific limits for equipment accuracy are provided and major sources for errors in measuring SDI are indicated.

2. Theory and background

A mathematical model was developed to describe the relation between SDI, particle concentration, and the test conditions under different fouling mechanisms. This developed model was used to study the influence of the membrane resistance and test conditions on the SDI values.

2.1. SDI definition

The SDI value is defined as:

$$\mathrm{SDI} = \frac{100\%}{t_\mathrm{f}}\left(1-\frac{t_1}{t_2}\right) = \frac{\%P}{t_\mathrm{f}} \qquad (1)$$

where t_1 is the time required to collect the first volume (500 ml for a 47 mm membrane); t_2 is the time required to collect the second volume (500 ml) and t_f is the time of the second measurement (15 min). If the plugging ratio (%P) exceeds 75%, a shorter period t_f has to be taken, for example 10, 5 or 2 min.

2.2. Fouling model

Hermia described four empirical models that correspond to four basic types of fouling: complete blocking, standard blocking, intermediate blocking, and cake layer formation [20].

The parameters considered by these models have a physical meaning and contribute to the comprehension of the mechanisms of membrane fouling. These models were developed for dead-end filtration and are based on constant pressure filtration laws. These fouling models are summarized in Table 1, where:

w_R represents the specific cake resistance and is defined as the volume of feed water per unit area for which the cake resistance is equal to the membrane resistance.
w_A represents the pore blocking potential and is defined as the volume of feed water per unit area that contains enough particles to block the pores completely.
w_v represents the pore filling potential and is defined as the amount of feed water per unit area that contains enough particles to fill the pores completely.

In previous work, we developed a mathematical model to determine the filtrated volume V as a function of the filtration time t [22]:

$$V(t)=\begin{cases} \dfrac{A_\mathrm{M}\cdot R_\mathrm{M}^{1-m}}{C\cdot(1-m)}\left(\left(1+\dfrac{(2-m)\cdot C\cdot \mathrm{d}P\cdot R_\mathrm{M}^{m-2}t}{\mu}\right)^{\frac{1-m}{2-m}}-1\right), & m\neq 1,2 \\ A_\mathrm{M}\cdot w_\mathrm{A}\,\ln\left(1+\dfrac{\mathrm{d}P\cdot t}{w_\mathrm{A}\cdot\mu\cdot R_\mathrm{M}}\right), & m=1 \\ A_\mathrm{M}w_\mathrm{A}\left(1-e^{-\frac{dP\cdot t}{w_\mathrm{A}\cdot\mu\cdot R_\mathrm{M}}}\right), & m=2 \end{cases} \qquad (2)$$

Table 1
Definitions of the four fouling mechanisms. The parameters m and C relate to the fouling mechanisms and particle concentration. Total resistance is a function of filtration state w [21]

Details	Definitions	m	C
Cake filtration	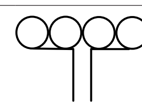	0	$\frac{R_\mathrm{M}}{w_\mathrm{R}}$
Intermediate blocking	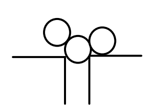	1	$\frac{1}{w_\mathrm{A}}$
Standard blocking	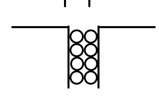	1.5	$\frac{2}{w_\mathrm{V}R_\mathrm{M}^{1.5}}$
Complete blocking	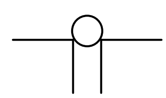	2	$\frac{1}{w_\mathrm{A}R_\mathrm{M}}$

The time t to collect filtration volume V can be calculated by inverting Eq. (2):

$$t(V)=\begin{cases}\dfrac{\mu}{(2-m)\cdot C\cdot \mathrm{d}P\cdot R_{\mathrm{M}}^{m-2}}\left(\left(\dfrac{V\cdot C\cdot(1-m)}{R_{\mathrm{M}}^{1-m}\cdot A_{\mathrm{M}}}+1\right)^{\frac{2-m}{1-m}}-1\right), m\neq 1,2\\ \left(e^{\frac{V}{w_{\mathrm{R}}\cdot A_{\mathrm{M}}}}-1\right)\cdot\dfrac{R_{\mathrm{M}}\cdot w_R\cdot\mu}{\mathrm{d}P},\ m=1\\ \ln\left(\dfrac{A_{\mathrm{M}}\cdot w_{\mathrm{A}}}{A_{\mathrm{M}}\cdot w_{\mathrm{A}}-v}\right)\cdot\dfrac{R_{\mathrm{M}}\cdot w_{\mathrm{A}}\cdot\mu}{\mathrm{d}P},\ m=2\end{cases} \tag{3}$$

Eqs. (2) and (3) can be combined to give an analytical expression for the SDI, which is not shown here as the expression is rather large [22].

2.3. Sensitivity and error analysis

2.3.1. Equipment accuracy and uncertainty

Accuracy of equipment is how close the measured value is to the true or actual value, while the error is the difference between these two values. Inaccuracy in the equipment leads to an error in the obtained SDI values. The error in SDI due to the inaccuracy in the equipment is calculated as follows:

$$\Delta\mathrm{SDI}=\frac{\partial\mathrm{SDI}}{\partial(\mathrm{parameter})}\times\Delta(\mathrm{Equipment\ accuracy}) \tag{4}$$

where ΔSDI is the error in SDI; ∂SDI/∂(parameter) is the change in SDI due to the variation in the testing parameter and Δ(Equipment accuracy) is the accuracy of the equipment used to measure the testing parameter.

The equipment used in the lab SDI setups (*see* Fig. 2(a) and (b)) have a limited guaranteed accuracy in measuring the testing condition parameters. The equipment inaccuracy is a result of the accuracy of the manufactured equipment and the operator's accuracy in using the equipment and monitoring the test conditions. The accuracy of the flow meter, thermometer, beaker, pressure sensor and the stopwatch are mentioned in the products' brochures. Lack of operator experience causes additional errors in the measurement of temperature, sample volumes, the times t_1 and t_2, and the time to start collecting the second sample t_f. The temperature in the field can easily vary from morning to night with ±5°C causing differences in SDI for the same feed water.

The equipment accuracy, operator error and the testing conditions are shown in Table 2. The operator errors are estimations based on our practical experience.

Table 2
Equipment used for the SDI test accuracy in the lab and in the field

Equipment uncertainty	Variation	
	Lab equipment	Field equipment
Equipment accuracy		
Flow meter	0.1 l h^{-1}	
Thermometer	0.1°C	0.1°C
Volumetric flask	0.25 ml/500 ml	
Pressure sensor	0.07 bar	0.1 bar
Stopwatch	0.01 s	0.01 s
Operator experience		
Thermometer	1°C	1°C
Beaker	5 ml/500 ml	50 ml/500 ml
Stopwatch in measuring t_1, t_2	2 × 0.5 s	2 × 2.5 s
Stopwatch in measuring t_{15}	10 s	15 s
Testing conditions		
Thermometer	1	5°C

In the field, fairly inaccurate equipment results in erratic SDI results. The error in V and t are relatively large for the field tests. This is caused by the fact that the operator has to start/stop the collection of permeate and start/stop the stopwatch at the same moment. Although according to the ASTM standard the water temperature T should remain constant (±1°C) throughout the test, in fact the SDI should be measured at a standard temperature. Mathematical and experimental results show that SDI values is very dependent on temperature. During field tests, a difference of 5°C is not unusual, depending on for example at what time during the day the SDI was performed.

2.3.2. Systematic error

Systematic errors in SDI test observations usually originate from unknown measuring equipment errors such as the support plate in the filter holder, height difference between the pressure gauge and the membrane, contamination in the membrane upstream, and errors in calculating the effective membrane area. Systematic errors can be difficult to identify and correct. Given a particular experimental procedure and setup, it does not matter how many times the experiment is repeated; the systematic error remains unchanged. No statistical analysis of the data set eliminates a systematic error, nor alerts us to its presence. A systematic error can be located and minimized with careful analysis and design of the test conditions and procedures, by comparing the results to other results obtained independently, or by using different equipment or techniques.

2.3.3. Artifacts

Errors appear in the SDI results which are not a true feature of the testing parameters, but instead are a result of experimental or observational mistakes. There are numerous examples of this. Gas bubbles can appear in the feed water which interrupt the filtration process and cause a high SDI value. The feed pump and the valves placed before the membrane can affect the particle size due to the shear force they exert on the particles. Carbon particles can be introduced in the feed solution originating from the graphite gear of the gear pump.

2.4. Influence of water salinity and acidity

SDI as a fouling index is related to the interaction between particles and the membrane, which is influenced by the water salinity and acidity. The initial rate of particle deposition depends on the colloidal interaction forces between particles and membrane surfaces, among which double layer forces are the most important. The double layer forces between particles, and between the membrane surface and the fouling are determined by the zeta potentials of particles and membranes, and by solution chemistry.

The AKP-15 particle which was used to prepare the model water has an iso-electric point (IEP) at pH 9 [23], while test membrane M7 has an IEP at pH 2.5–3 [24]. Therefore, the particles and membranes are oppositely charged in the range of pH 2.5–9.

The particles deposit on the membrane surface as a cake or are adsorbed on the internal pore surface causing pore blocking. At $SDI_O = 3$, cake filtration dominates the fouling mechanisms and most of the particles are deposited on the membrane surface. At high ionic strength, the interaction double-layer forces between the particles and the membrane surface are small because of double layer compression. As a result, particles, which are transported to the membrane surface by the inherent permeation drag, deposit onto the membrane or inside the pore. No significant lateral repulsion occurs between deposited particles, so their density on the membrane surface is relatively high. Because the particles are unstable at a high ionic strength, the deposition of suspended particles onto previously retained particles is also favorable. This deposition behavior results in a thick fouling layer and extensive fouling. Therefore, a high ionic strength of the test water may result in increasing SDI values.

At low ionic-strength, the initial deposition of particles onto the oppositely charged membrane surface is favorable. Because of the low ionic strength, strong lateral double-layer repulsion exists between retained particles, and the initial density of surface coverage is not too high. Under these conditions, strong double layer repulsion also exists between retained particles and approaching suspended particles. In this case, the extent of colloidal fouling is postulated to depend on the interplay between double-layer repulsion and permeation drag [25–28].

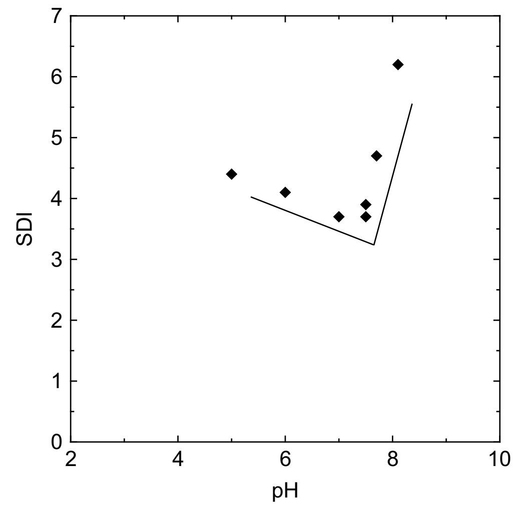

Fig. 1. SDI values versus pH of UF seawater (Redrawn from Ref. [29]).

The effect of pH on SDI for seawater was discussed by Mosset et al. [29]. Their SDI results as function of pH are plotted in Fig. 1.

Fig. 1 shows SDI values increasing from 4 to 6 when the pH is increased from 7 to 8. Mosset et al. stated that this is mainly due to dissolved substances (Ca, Mg,…) which precipitate with increasing pH. Moreover, the pH influences the double-layer forces between particles and the membrane surface.

3. Material and methods

In this section, the procedure for measuring the SDI using the lab scale SDI setup is described. The MF membrane and model feed water are listed, and the reference testing conditions are defined. Besides that, the particle size distribution measurement protocol is also described.

3.1. SDI setup

Fig. 2 shows the two setups used for the SDI tests. The applied pressure was maintained either by the feed pump (Fig. 2(a)) in the automatic setup or by pressurized gas N_2 (Fig. 2(b)) in the manual setup. The feed flow is

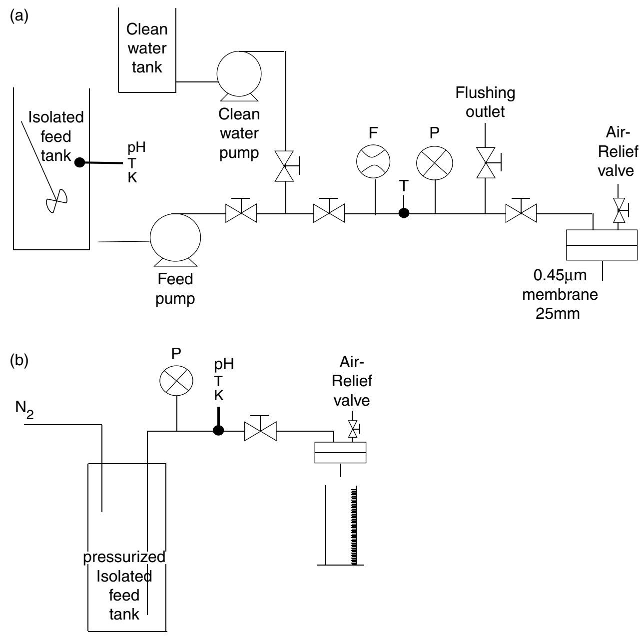

Fig. 2. Flowsheet of the SDI setup. (a) Automated SDI setup using a feed gear pump. (b) Manual SDI setup using a feed tank pressurized by N_2. Feed tank is shown. pH, temperature (T) and conductivity (K) are measured in the feed tank. Pressure (P), flow rate (F) and temperature (T) are measured in the feed line.

automatically controlled to supply a constant feed pressure. The feed tank was isolated to keep the water temperature constant (±1°C) throughout the tests. The flow rate, pressure and temperature were measured. An MF 0.45 µm membrane filter (25 mm in diameter) was placed on the support plate of the holder. The membrane filter was touched only with tweezers to avoid puncturing or contamination. It was checked whether the O-ring was in a good condition and properly placed. The trapped air was bleed out through a relief air valve in the filter holder. Before installing the membrane filter, the water to be tested was flushed through the apparatus in order to remove entrained contaminants. The times to collect the first sample (141 ml) and the second sample (141 ml) after 15 min total elapsed flow were calculated using the collected filtration data.

From the raw data generated by the SDI setup, the resistance and filtered volume were calculated. Then C, m and R_M were determined by least-squares curve fitting [30], which minimizes the following error criterion:

$$\min \sum_{i=0}^{n} (f(w_i, R_\mathrm{M}, C, m) - R_i)^2 \tag{5}$$

where n is the number of data points; W_i is the accumulated filtrated volume per unit area and R_i is the total resistance at data point i.

3.2. Membrane

Eight 0.45 µm MF membranes were chosen for this study (Table 3), including three membrane filters meeting the ASTM standard (M4, M6, and M7).

For surface SEM images, a dry sample was sputtered with a very thin gold layer (SCD040, Blazers Union). The samples were dried overnight in a 30°C oven under vacuum.

Up to 50% variation was observed in the overall membrane properties (e.g., pore size, porosity) for membranes M1–M8 [15]. The membrane resistance R_M of M1 varies 23% within the same batch of membranes, while M7 has only 7% variation in the membrane resistance R_M [15]. The variation in the membrane properties causes different SDI results for the same water quality. The membrane resistance was considered as a representative parameter of most of the physical membrane properties such as the pore size and the porosity. However, other membrane properties such as surface charge, also influence the adsorption of nano-particles.

3.3. Colloidal suspension as model water

To prepare the model feed water, hydrophilic α-alumina particles (AKP-15, Sumitomo Chemical, Tokyo, Japan) with a core particle size of 0.6 µm and an isoelectric point (IEP) at pH 9 [23] were used. The AKP-15 particles have a narrow size distribution curve. The feed solution was prepared by adding 4 mg l^{-1} AKP-15 to demineralized water, purified by an Ultra-Pure system from Millipore (Synergy SYNS). The solution was well-mixed using a mechanical mixer in the feed tank.

Table 3
Microfiltration membranes used in this work. Pore size as given by manufacturer. R_M is the average measured clean water resistance (20°C) [24]

Code	Material	Nominal pore size [µm]	R_M [$\times 10^{10}$ m^{-1}]
M1	PVDF	0.45	0.83
M2	PTFE	0.45	0.41
M3	Acrylic polymer	0.45	0.66
M4	Nitro cellulose[1]	0.45	0.64
M5	Nylon6,6	0.45	2.65
M6	Cellulose acetate[1]	0.45	0.74
M7	Cellulose acetate[1]	0.45	0.85
M8	Polycarbonate	0.45	0.39

[1]ASTM standard material.

A Malvern Instruments, Zetasizer range with Dynamic light scattering (DLS) was used to measure the α-alumina particle size distribution. To avoid the agglomeration of the particles, the pH was adjusted to 4.1 by adding HNO_3

3.4. Defined reference testing conditions

Membrane resistance, feed temperature, applied pressure and the membrane area are the main testing conditions in this study. In order to study the effect of each parameter independently, the reference testing conditions were defined and summarized in Table 4.

a. The membrane resistance R_M:
   In the 2007 updated version of the ASTM standard, the membrane filter was further specified. The pure water flow time should be 25–50 sec/500 ml under an applied pressure 91.4–94.7 kPa. The calculated membrane resistance R_M then is in the range 0.86×10^{10} to 1.72×10^{10} m^{-1}. An average value of $R_M = 1.29 \times 10^{10}$ m^{-1} is chosen as the reference membrane resistance.
b. Feed temperature T:
   Based on the lab temperature, $T_o = 20$°C was used as reference feed temperature.
c. Applied pressure dP:
   The ASTM standard applied pressure dp_o = 207 kPa was defined in this study as the reference pressure.
d. Membrane area A_M:
   A diameter of 47 mm was considered as the standard membrane size and therefore the reference membrane area $A_{Mo} = 13.4 \times 10^{-4}$ m^2.
e. SDI_O:
   The SDI limitation for the RO feed water $SDI_O = 3$ was taken as a target value.
f. $w_{R,A,V}$:
   The fouling potentials (cake filtration, intermediate, standard and complete blocking) of the feed water all correspond to $SDI_O = 3$.

Table 4
Reference testing conditions

Parameter	Reference value
R_{MO}	1.29×10^{10} m^{-1}
t_o	20°C
dP_o	207 kPa
A_{MO}	13.4×10^{-4} m^2
SDI_O	3
W_{RO} (Cake filtration)	12.2
W_{AO} (Intermediate pore blocking)	17.5
W_{VO} (Standard pore blocking)	40.5
W_{AO} (Complete pore blocking)	24.3

Table 5
Modeling input values for different testing conditions and their variation range

Parameter	Reference value	Variation range to be studied
R_M	1.29×10^{10} m^{-1}	0.39×10^{10}–2.65×10^{10} m^{-1}
dP	2.07×10^5 Pa	50–400 kPa (0.5–4 bar)
A_M	13.4×10^{-4} m^2	
$V_{1,2}$	500 ml	
t_f	15 min	
T	20°C	5–70°C
MFI		0–3.5 s l^{-2}

3.5. Modeling input data

The above input data were used to mathematically study the sensitivity of SDI for errors (Table 5).

The water viscosity was calculated using the following empirical equation[31,32]:

$$\mu = 0.497 \times (T + 42.5)^{-1.5} \tag{6}$$

where T is the water temperature (°C).

4. Results and discussion

4.1. Deviation ±0.1 at $SDI_O = 3$

There is no allowable error mentioned for the SDI test in the ASTM standard or in literature. From a practical point of view and based on our experience, a deviation of 0.1 in the SDI result can be acceptable. Assuming cake filtration and the reference testing conditions mentioned in Table 4, the variations of several testing parameters resulting in a deviation of ±0.1 at $SDI_O = 3$ are calculated. Table 6 shows this variation for each testing condition (T, dP, R_M, A_M and the times t_1, t_2 and t_f).

Table 6
Variation range in the testing parameters resulting in a deviation $SDI_O = 3 \pm 0.1$ for a cake filtration mechanism

Parameter	SDI = 3	SDI = 3 ± 0.1
T [°C]	20	23.36–16.84
dP[kPa]	207	224–192
R_M[m^{-1}]	1.29×10^{10}	1.19×10^{10}–1.40×10^{10}
A_M[m^2]	1.39×10^{-3}	$>2.63 \times 10^{-4}$
t_1 [s]	22.96	22.33–23.58
t_2[s]	41.74	42.92–40.60
t_f [min]	15 min (900 s)	871.2–931.2 s

Table 6 shows that an error of ±0.6 sec in measuring the time to collect the first sample (t_1) results in a ±0.1 variation of the SDI value. However, the variation in measuring the time to collect the second sample t_2 for obtaining an identical ±0.1 variation in SDI value is twice that in t_1, ±1.18 sec. Under cake filtration, the relationship between the total resistance R and the filtrated volume V is linear. Due to the linearity between R and V, the error in measuring the membrane area results in an increase in both sampling time t_1 and t_2 with almost same ratio. Thus, an increase in the membrane area A_M does not have an effect on the SDI value, whereas decreasing A_M has a small effect and SDI remains almost constant. Collecting the second sample should start after an elapsed filtration time t_f of 15 min. However, the collection of the second sample can be earlier or later due to an error in measuring the 15 min. An error of +30 or −70 sec in measuring t_f causes a ±0.1 deviation in the measured SDI value.

From Table 6, we conclude that SDI is more sensitive for errors in measuring t_1 and t_2, while SDI is hardly sensitive for inaccuracies in the membrane area A_M in the case of a cake filtration mechanism.

4.2. Equipment accuracy and uncertainty

Errors due to inaccuracies in the equipment readouts can result in erratic SDI results. There is a large variation of equipment on the market which can be used for SDI testing in terms of quality and price. The manual equipment selected for field use is most likely to be lower in accuracy and price compared to lab equipment. Besides that, a wide range of commercial membranes with a pore size of 0.45 μm are available which can be used for the SDI test. The errors in the SDI results due to the variation in the testing conditions due to the inaccuracy of the used equipments and the membrane resistance are discussed in this work.

4.2.1. Different fouling mechanisms

The sensitivity of SDI for errors in measuring temperature, applied pressure and membrane resistance were studied for the four different fouling mechanisms. The effect of the equipment accuracy and errors on the SDI value was calculated by substituting the mathematical SDI model (Eqs. (2) and (3)) in Eq. (4).

The accuracy values in Table 2 for lab equipment were used to compare the SDI sensitivity for errors for the four different fouling mechanisms. The ASTM standard allows a ±7 kPa error in the applied pressure and a variation of 1°C in the temperature [33]. The error in the membrane resistance was estimated to be 0.1×10^{10} m^{-1}. Fig. 3 shows the errors in the SDI due to the inaccuracy of the equipment in measuring T and dP and the membrane resistance R_M. For cake filtration mechanisms, the fouling potential index I was assumed to be equal to 1.056×10^9 m^{-2}, corresponding to $SDI_O = 3$. In Fig. 3 the variation in the SDI results due to the variation in each parameter for the four fouling mechanisms are presented by the error bars.

The effects of a variation in the different testing conditions on the SDI can be studied in Fig. 3 by comparing the graphs horizontally. Fig. 3 shows that the SDI is more sensitive for errors in the membrane resistance than for errors in the temperature and the applied pressure. The SDI is more sensitive for errors during the test when a membrane with a low resistance is used, when a lower pressure is applied, or when the test is performed at a low temperature. By comparing the graphs in Fig. 3 vertically, we can conclude that the effects of different fouling mechanisms on SDI sensitivity are negligible. As simplification for the calculations, in the next sections therefore a cake filtration mechanism is assumed.

4.2.2. Accuracy of the SDI equipment

The minimal requirements for the accuracy of SDI equipment are not specified at all in the ASTM standard. As a result, equipment with a low accuracy is often used to measure the SDI, and this, in turn, leads to erratic SDI results. In this section, the different components of the SDI equipment are examined for their inaccuracy and their effect on the SDI results.

4.2.2.1. Feed temperature (thermometer) In the most recently ASTM standard, no reference temperature was suggested for measuring or correcting SDI. The flow rate through the membrane is affected by variations in the feed water temperature. SDI values obtained at different feed water temperatures may not necessarily be comparable [33]. An inaccuracy in the thermometer of ±1°C is estimated for the calculations. In Fig. 4, SDI values were plotted as a function of the specific cake resistance to simulate varying particle concentrations, and assuming a feed temperature of 20 ±1°C. The SDI sensitivity for errors in measuring the temperatures is calculated by substituting the mathematical SDI model of Eqs. (2) and (3) in Eq. (4). From Fig. 4 we can conclude that the effect of a ±1°C error in measuring the temperature only has a very small effect on the SDI results.

4.2.2.2. Applied pressure "pressure gauge" ASTM allowed a variation of ±0.07 bar (1 psi) in measuring the applied pressure during the SDI test. Two pressure indicators with an accuracy of ±0.07 bar and ±0.1 bar were used in the error calculations for the lab and field measurements, respectively. The SDI values were plotted in Fig. 5(a) and (b) as a function of the specific cake resistance assuming applied pressures of 207±7 and

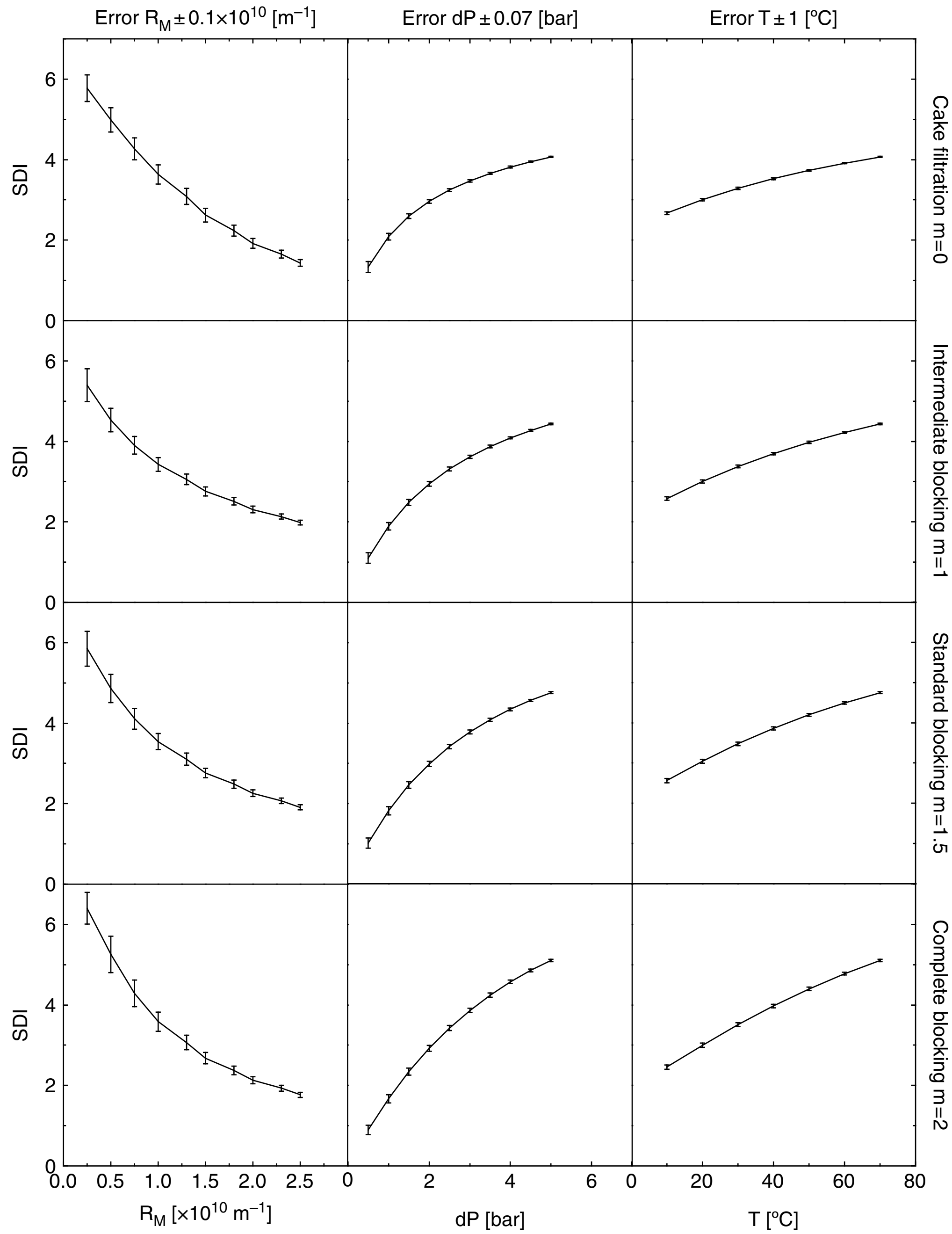

Fig. 3. Accuracy errors in equipment and membrane resistance under different fouling mechanisms.

207±10 kPa. The effect of the error in measuring the applied pressure was calculated by substituting the SDI model described by Eqs. (2) and (3) in Eq. (4). The effect of a ±0.07 bar and ±0.1 bar error on the SDI results was small and negligible.

4.2.2.3. Membrane area A_M The O-ring in the filter holder covers part of the membrane surface. The covered part of the membrane is inactive for filtration. The error in measuring the membrane diameter for different types of filter holders was experienced to be ±2 and ±4 mm for a 47 mm membrane diameter for the lab and field equipment, respectively. This causes an error in the membrane area A_M of ±8.3 % and ±16.3 %. The specific cake resistance R_C was varied between 0.01 and 1×10^{10} m^{-2}. The effect of ±8% and ±16.3% errors in the membrane area on the SDI results was determined by using Eqs. (2)–(4) and assuming cake filtration. The results are shown in Fig. 6(a) and (b). The influence of ±8.3% and ±16.3% errors in calculating the membrane area

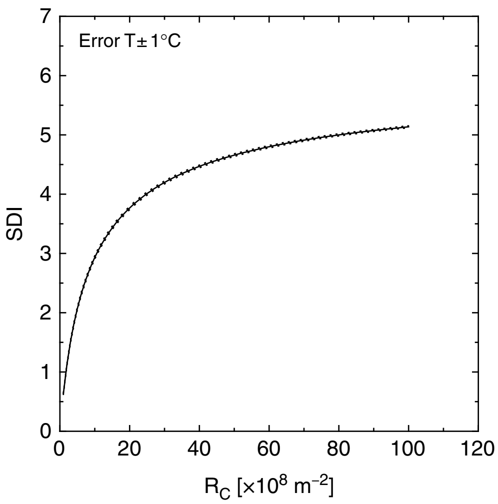

Fig. 4. Effect of an accuracy error in T on the SDI variation (dotted lines) under cake filtration at 20 ±1°C as a function of the specific cake resistance.

are close to zero. The sensitivity of SDI for an error in measuring A_M therefore is negligible.

4.2.2.4. Timing (stopwatch) An error in the stopwatch will have an effect on the determination of t_1, t_2 and t_f and consequently in the calculation of SDI using Eq. (1). To study this effect, as an illustrative example the following assumptions were made: the errors in t_1 were ±1 and ±5 s (lab and field equipments), t_1 varied between 20 and 200 s, and t_2 was 200 s. SDI results and the effect of ±1 and ±5 s errors in t_1 are presented in Fig. 7. The first derivative of Eq. (1) with respect to t_1 describes the change in the SDI due to an error in $t_1$as shown in Eq. (7):

$$\Delta \mathrm{SDI} = \pm\left(\frac{100}{t_2 \times t_f} \times \Delta t_1\right) \tag{7}$$

where, t_f = 15 min, t_2 = 200 s, Δt_1 error in measuring t_1 = 1 or 5 s. The SDI variation is not influenced by the value of t_1, and ΔSDI is equal to ±0.03 and ±0.17 respectively.

The effect of an error in measuring t_2 on the SDI results was studied assuming the errors in t_2 to be ±1 and ±5 s (lab and field equipment, respectively) for t_2 between 20 and 200 s, and t_1 equal to 20 s. The first derivative of Eq. (1) with respect to t_2 describes the effect of the error on the SDI as shown in Eq. (8):

$$\Delta \mathrm{SDI} = \pm\left(100 \times \frac{t_1}{t_f \times t_2^2} \times \Delta t_2\right) \tag{8}$$

where, t_f = 15 min, t_1 = 20 s, Δt_2 error in measuring t_2 = 1 or 5 s. The SDI results and the effect of ±1 and ±5 s errors on t_2 are shown in Fig. 8.

The sensitivity of the SDI for errors in measuring t_2 is increasing with decreasing SDI. The SDI can even have a negative value due to an error in measuring t_2, as shown by the SDI values between −1.5 and 1.8 due to a 5 s error in measuring t_2 when t_1 equals 20 s. The effect of 1 and 5 s errors on the SDI variation resulted in a ΔSDI decreasing from ±0.33 and ±1.7 down to zero,

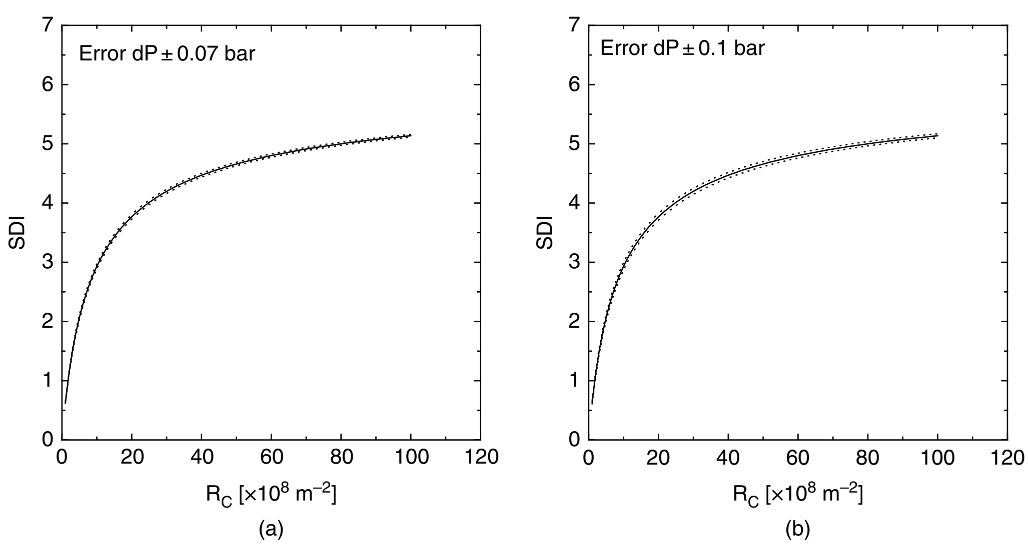

Fig. 5. Effect of an accuracy error in dP determination on the SDI variation (dotted lines) under cake filtration at 207 kPa as a function of the specific cake resistance. (a) ±7 kPa; (b) ±10 kPa.

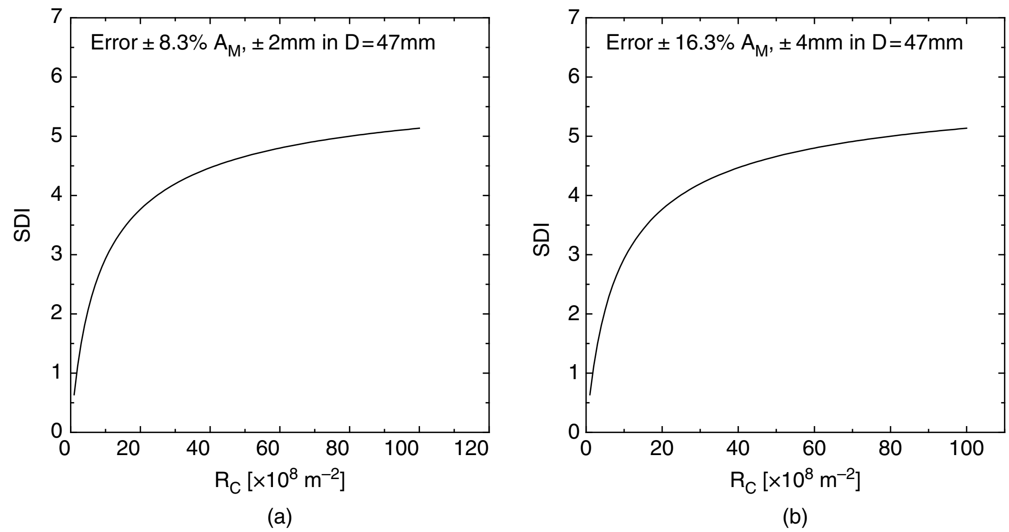

Fig. 6. The effect of (a) 8.3% and (b) 16.3% error in the membrane area on SDI as a function of R_c under a cake filtration mechanism.

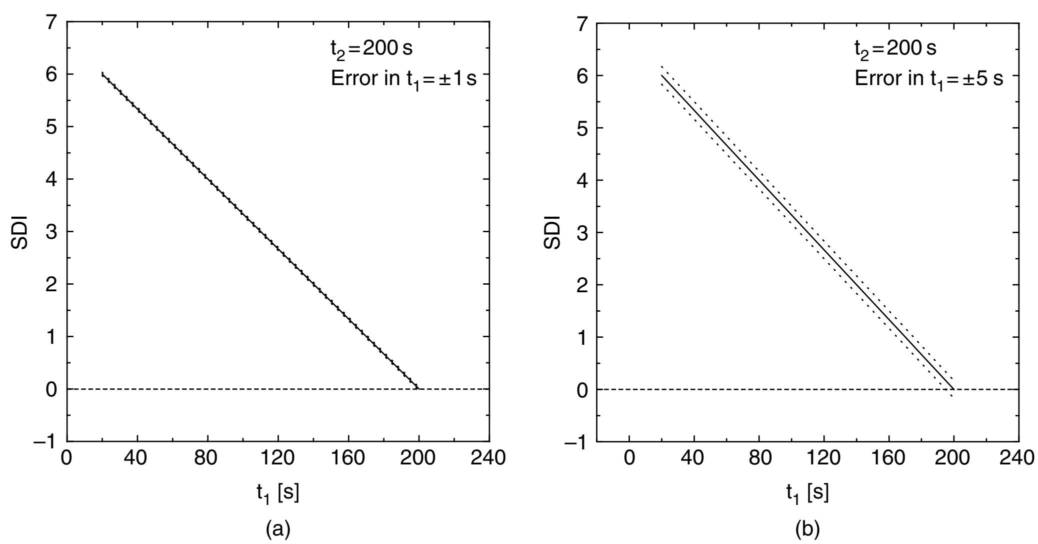

Fig. 7. The effect of an accuracy error in t_1 on the SDI variation (dotted lines) under cake filtration for t_2 = 200 s as a function of t_1. (a) ±1 s; (b) ±5 s.

respectively, with increasing SDI (increasing t_2). The SDI sensitivity for errors in t_2 was significant and the larger the error in t_2 and the lower the SDI, the more sensitive the SDI is.

The error in the elapsed filtration time t_f after starting the measurement (usually 15 min) was experienced to be ±10 to ±15 s. The feed water quality was changed by varying the specific cake resistance R_C between 0.01 and 10^{10} m^{-2}. The effect of the ±10 and ±15 s errors on the variation of the SDI was calculated using Eq. (9).

$$\Delta \mathrm{SDI} = \pm\left(\frac{100}{t_f^2} \times \left(1 - \frac{t_1}{t_2}\right) \times \Delta t_f\right) \tag{9}$$

where, t_1 = 20 s; t_2 = 200 s; Δt_f error in measuring t_f = 10 or 15 s. The results were plotted in Fig. 9. The assumed errors in t_f have a maximum effect on the SDI of ±0.05 and ±0.07, respectively.

4.2.2.5. Sample volume determination (volumetric flask) The 500 ml sample volume was based on using

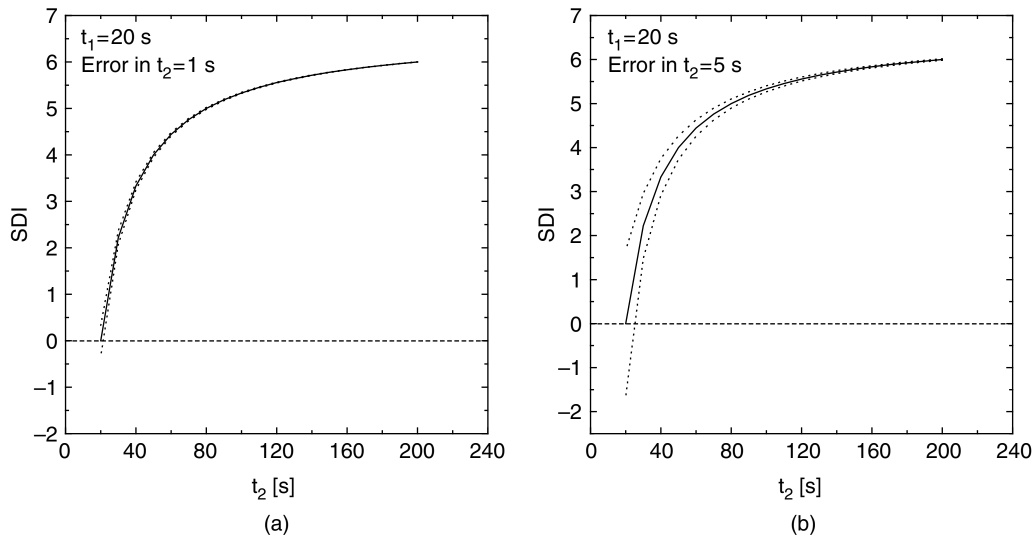

Fig. 8. The effect of an accuracy error in t_2 determination on the SDI variation (dotted lines) for t_1 = 20 s as a function of t_2 assuming cake filtration. (a) ±1 s; (b) ±5 s.

a 47 mm diameter membrane. In the lab, a volumetric flask was used to measure the sample volumes V_1 and V_2. We experienced that the flask manufacturing accuracy and operator errors together in the lab and field can sum up to ±5 ml/500 ml and ±50 ml/500 ml per volume measurement respectively. The effect of the flask errors on ΔSDI were calculated using Eq. (10) and plotted in Fig. 10 as a function of the specific cake resistance. The maximum SDI sensitivity for 5 ml/500 ml and 50 ml/500 ml errors in the sample volume were ±0.003 and ±0.6, respectively.

$$\Delta \mathrm{SDI} = \frac{\partial \mathrm{SDI}}{\partial V_1} \times \Delta V + \frac{\partial \mathrm{SDI}}{\partial V_2} \times \Delta V \tag{10}$$

4.2.3. Membrane resistance

The membranes M1–M8 previously tested show a wide range of membrane resistances R_M (0.39×10^{10}–2.65×10^{10} m^{-1}) [15]. The requirement of the ASTM standard is $0.86 \times 10^{10} < R_M < 1.72 \times 10^{10}$. This broad range of allowable membrane resistances explains, at least partly, the frequently reported erratic SDI results. The effect of a

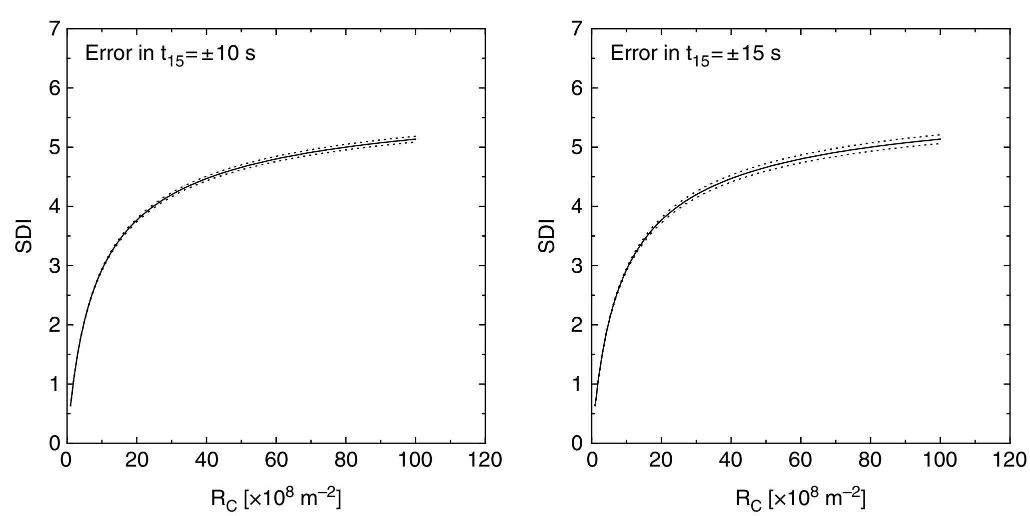

Fig. 9. The effect of an accuracy error in t_f on the SDI variation (dotted lines) under cake filtration for t_1 = 20 s and t_2 = 200 s as a function of R_c. (a) ±10 s; (b) ±15 s.

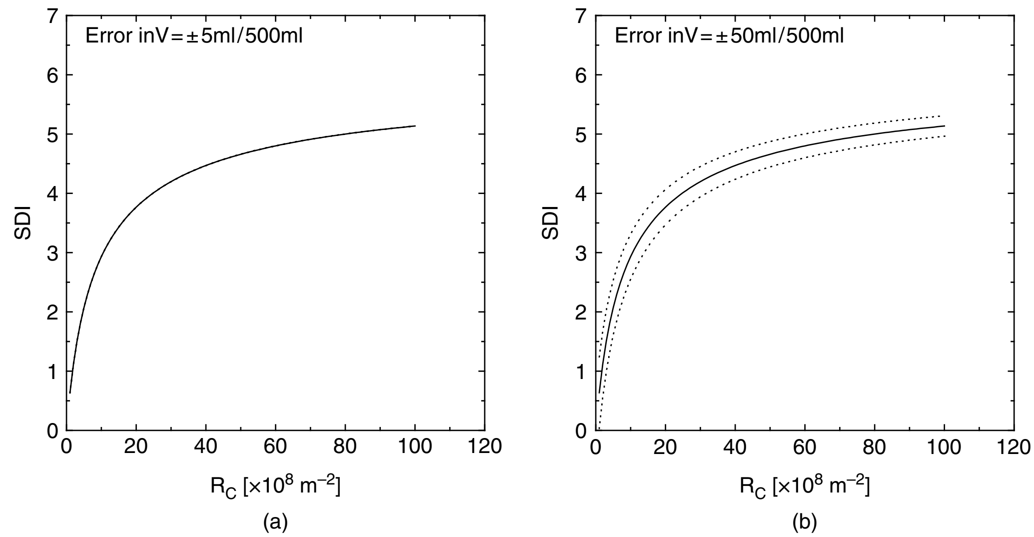

Fig. 10. The effect of an accuracy error in the determination of V on the SDI variation (dotted lines) under cake filtration as a function of R_c for V = 500 ml. (a) ±5 ml; (b) ±50 ml.

variation in the membrane resistance on the SDI results was calculated using Eqs. (2)–(4) assuming the reference testing conditions in Table 4. The error in the reference membrane resistance R_{MO} was estimated to be ±10%. The SDI results were plotted in Fig. 11.

Fig. 11 shows that the guidelines indirectly set by ASTM for the resistance of the used membranes are much too broad resulting in a maximum variation of 2.29–3.98 at SDI = 3 for a membrane with a resistance R_{MO} (1.29×10^{10} m^{-1}). To avoid this deficiency of the SDI test, it is recommended to narrow the allowable range to 10% of the R_{MO} value 1.29×10^{10} m^{-1} which reduces the error to only ±0.25 at SDI_O = 3.

To experimentally demonstrate the influence of the membrane resistance on SDI, eight different membranes with different clean water resistances as described in Table 3 were used. The feed solution of 4 mg l^{-1} α-alumina particles (AKP-15) was prepared in a big feed tank to maintain a constant feed water quality during all experiments. SDI tests were performed at a temperature of 20°C. The applied pressure was kept constant at 207 kPa. SDI results were plotted versus the membrane resistance in Fig. 12.

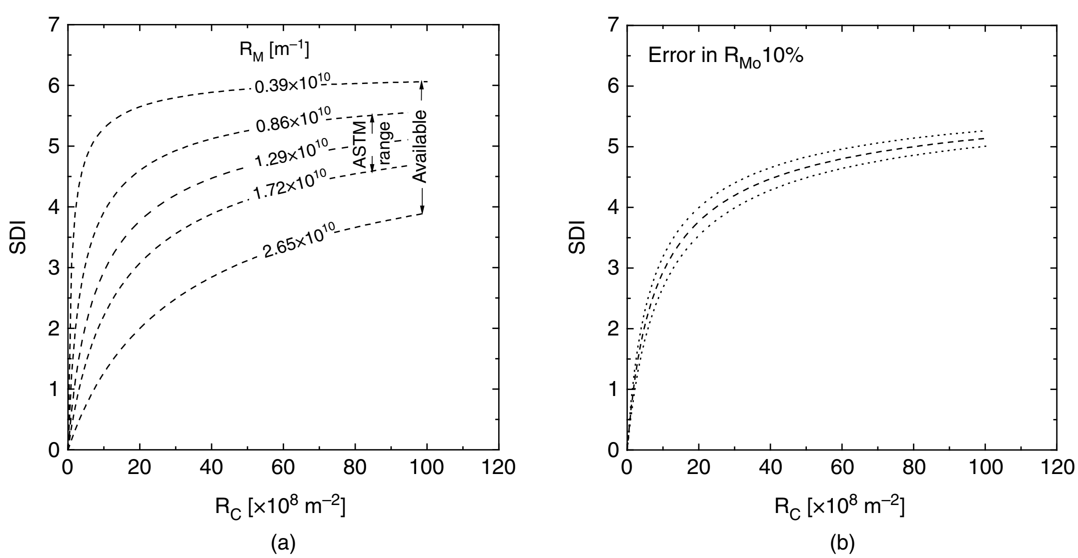

Fig. 11. The effect of the membrane resistance on SDI as a function of RC, assuming a membrane area (AM) 13.8×10^{-4} m^2, temperature (T) 20°C and pressure (dP) 207 kPa. ASTM range: 0.86×10^{10} to 1.72×10^{10}. Tested range M1–M8: 0.39×10^{10} to 2.65×10^{10} m^{-1}; (b) the effect of ±10% variation in RMO (1.29×10^{10} m^{-1}).

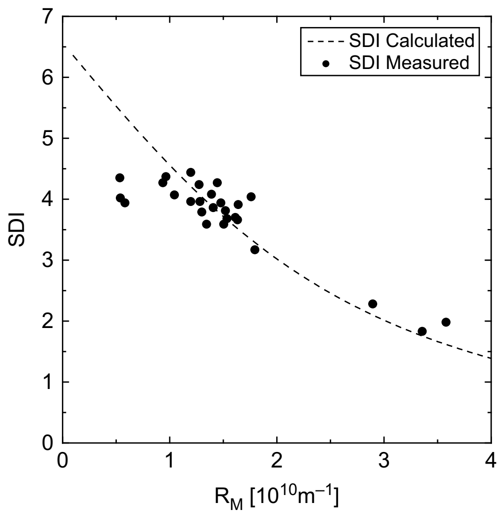

Fig. 12. Experimental and theoretical SDI results as a function of the membrane resistance for different membranes. The experiments were carried out using a particle concentration of 4 mg l^{-1} AKP-15 and a pressure difference of 207 kPa.

The experimental results show that the SDI decreases with an increase in the membrane resistance R_M. An increase of the membrane resistance from 0.5×10^{10} m^{-1} to 3.5×10^{10} m^{-1} leads to a decrease in SDI from 4.5 to 2 for the same water quality.

4.2.4. Total error in the SDI due to inaccuracies

The total error in the SDI due to the inaccuracy in the equipment that can be used to measure SDI is the sum of all individual errors. The total error can be calculated by substituting the SDI model built with Eqs. (2) and (3) in Eq. (4) for each individual parameter:

$$\begin{aligned}\text{Total error} = &\left(\frac{\partial \text{SDI}}{\partial V_1}\times \Delta V\right)+\left(\frac{\partial \text{SDI}}{\partial V_2}\times \Delta V\right)+\left(\frac{\partial \text{SDI}}{\partial t_f}\times \Delta t\right)\\ &+\left(\frac{\partial \text{SDI}}{\partial A_M}\times \Delta A_M\right)+\left(\frac{\partial \text{SDI}}{\partial\, dP}\times \Delta P\right)+\left(\frac{\partial \text{SDI}}{\partial T}\times \Delta T\right)\\ &+\left(\frac{\partial \text{SDI}}{\partial R_M}\times \Delta R_M\right)+\left(\frac{\partial \text{SDI}}{\partial t_1}\times \Delta t\right)+\left(\frac{\partial \text{SDI}}{\partial t_2}\times \Delta t\right)\\ &+\left(\frac{\partial \text{SDI}}{\partial t_f}\times \Delta t\right)\end{aligned} \quad (11)$$

By substituting the variations mentioned in Sections 4.2.2. and 4.2.3. into Eq.(11), it can be concluded that for the lab equipment the SDI can vary with ±0.40, and for the field equipment with ±2.11.

4.2.5. Effect of a variation in membrane properties within a batch

Two membranes from two different manufacturers were tested to show the influence of variations in membrane properties within a batch on the SDI. The variations in the membrane resistances were 23% and 7% within one batch for M1 and M7, respectively [15]. Assuming the reference testing conditions listed in Table 4, the SDI sensitivity for the variation in membrane resistance were calculated by substituting the SDI model described by Eqs. (2) and (3) in Eq. (4). The SDI sensitivity is plotted in Fig. 13 as a function of the specific cake resistance.

At SDI = 3 for membrane M1, the SDI varied between 3.58 and 2.42 due to the variation in membrane resistance within one batch. This again illustrates the difficulties in reproducing the SDI in the field due to variations in the membrane resistance within one batch of the same test membrane.

4.3. Systematic errors

In this section the experienced practical errors, such as the effects of the pump and filter holder support plate, will be transformed into an error in the SDI results. Systematic errors in the SDI test were difficult to identify, separate and correct. Personal experience and mistakes during the duration of this project lead to the discovery of error sources, such as the filter holder, cleanliness of the setup, and level difference between the filter and the pressure gauge. The change in SDI due to the systematic errors was mathematically estimated using the SDI model built with Eqs. (2) and (3) and the reference testing conditions.

The filter holder components are the inlet, top cover, O-ring, support plate, and outlet. All of these components can be a source for errors. Some big objects in the feed water can partially block the holder inlet. The pressure gauge is located in the holder upstream. Therefore, additional resistance in the holder inlet leads to an error in the gauge readout and in the measured SDI. Assume SDI = 3, and that an error of 0.1 bar due to the blocking in the holder inlet was observed. As a result, the mathematically calculated SDI value varied between 3.06 and 2.94 assuming cake filtration.

The color of the membrane surface changes because of the deposit of foulants. An abnormal concentration of the deposited foulants can be observed as more intense color on the membrane surface. The support plate, located underneath the membrane to hold and support the membrane, can seal part of the membrane and lower the water flow. The effective membrane area in this case is smaller and the filtrated sample volume should be adjusted. When not corrected, this systematic

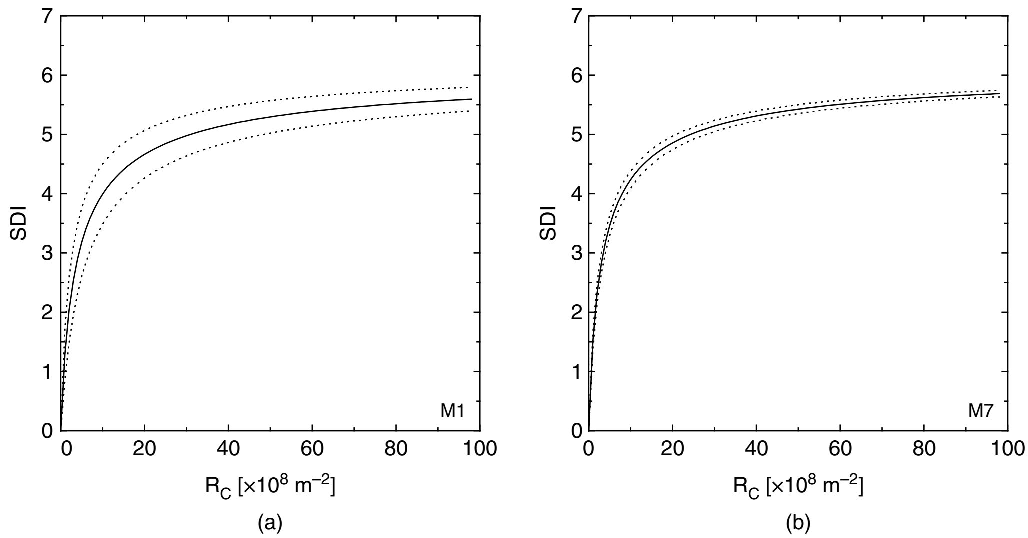

Fig. 13. The influence of the variation in R_M within a batch of membranes (a) M1 and (b) M7 on SDI. M1 clean membrane resistance R_M 0.85×10^{10} m^{-1} with a variation of 23%. M7 clean membrane resistance R_M 0.74×10^{10} m^{-1} with a variation of 7%.

error affects the SDI value since it is obtained with the wrong sample volume. Practically, up to 53% of a membrane surface area can be sealed by the support bulge (*see* Annex 1–4). Assuming that 53% of the pores will be also sealed in that case, the difference between the real effective membrane area and the assumed area causes an SDI drop from 3 to 2.98. To avoid the effect of the support plate, the use of a filter paper under the membrane is recommended.

Another error source influencing the estimation of the effective area is the O-ring. The O-ring is placed on the top of the membrane to seal the membrane in the cell. The O-ring minimizes the effectiveness of the membrane area as well. The thickness of the O-ring determines the covered area.

System cleanliness and contamination are one of the major sources of systematic errors in measuring an SDI. The SDI limit (SDI = 3) can be easily obtained with 4 mg l^{-1} particles (0.08 g particles in 20 l ultra-pure water with membrane M7). However, any small contamination present in the upstream leads to an increase in the SDI value. A 10% increase in the particle concentration (W_v decreases from 12.17 to 11.06), causes already an increase in SDI from 3 to 3.13.

The pressure gauge and the filter holder should be at the same level. A difference in level causes an additional pressure difference over the membrane. A level difference of 1 m between the pressure gauge and the filter holder, increases the SDI from 3 to 3.06.

The calculated effects of each of the above mentioned individual errors on SDI are very minimal. However, the accumulated effect of all the errors can have a larger impact on SDI.

4.4. Artifacts

During the SDI test, pressurized gas can be used to build up the driving force (pressure) in the feed tank. At the required pressure of 207 kPa, the feed water is super-saturated with gas compared to water at atmospheric pressure, and gas bubbles form during filtration. These gas bubbles obstruct the membrane pores and prevent the water from permeation through the membrane which decreases the flow through the membrane. Consequently, the fouling rate increases and SDI is higher. The effect of entrapped air on the MFI results was mentioned before by Dillon et al. [34].

In order to demonstrate the effect of gas bubbles on the SDI value, two SDI tests were performed using M7, the membrane with lowest variation in its properties. Sufficient feed solution containing 4 mg l^{-1} of AKP-15 particles was prepared and divided for two SDI tests. The first SDI test was performed in the morning. The feed solution for the second SDI test was stored under 400 kPa pressure overnight, resulting in an over-saturated feed solution. The next morning, the second SDI test was performed with new membrane out of the same M7 batch. In the second SDI test, gas bubbles clearly were observed upstream of the membrane and on the membrane surface as well. The SDI value increased from 3.31 to 3.80 solely due to the effect of the gas bubbles present in the feed water.

Particle size and nature might change due to the shear forces during mixing in the feed tank, and shear forces caused by the feed pump, flow meter and valves. Three samples were taken from the feed tank (top, middle and bottom of the tank). Three samples (triplicate) were also taken directly at the following positions: the feed pump,

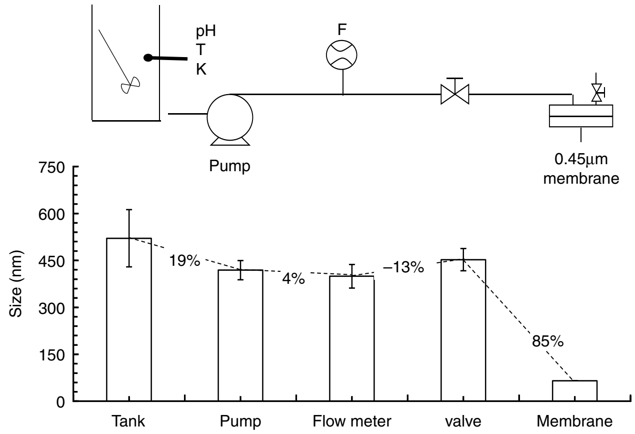

Fig. 14. Average particle size along the SDI setup. pH (5.6), temperature (T = 20°C) and conductivity (K = 180 µS cm^{-1}) were measured in the feed tank. The flow rate (F) measured with online flow meter. Membrane M7 was used in the filter holder.

the flow meter, the valve and the membrane. The results of the average measured particle size are presented in Fig. 14.

The particle size in the feed tank varied between 0.44 and 0.62 µm. The shear force in the feed pump lowered the particle size by 19%. Due to particle agglomeration caused by the shear force in the valve, the average particle size increased with 13%. At the membrane permeate side the average particle size was 100 nm. We can conclude that for this model water, the particle size in the membrane cell is the same as in the feed tank, within the error margins. These agglomeration/separation processes of course are dependent on the particle properties and the pH of the water, so this conclusion cannot be generalized.

Cavitations of the pump were experienced in the membrane fouling experiments of Dillon et al. [34]. Another pump effect is that wear of the gear pump can be a source for particles that arrive to the membrane surface. SDI tests with ultrapure water were performed using two gear pumps made of different material (graphite and PTFE). SEM images (top surface) of the used M7 membranes were taken after the SDI tests, as well as that of a virgin M7.

The SEM images in Fig. 15(a–c) show the top surface of the membrane and the deposited particles. The SEM images show that carbon particles introduced by the graphite gear were deposited on the membrane surface. Fig. 15 also shows that larger particles (>2 µm) deposited on the membrane surface, originating from the PTFE gear pump. The SDI for particle free, ultrapure water should be zero. However, SDI values were 0.31 and 0.24 for ultrapure water using the graphite and PTFE pump gears, respectively. Mathematically, this increase in the SDI values is equivalent to specific cake resistance R_C 4.5 × 10^7 m^{-2} and 3.4 × 10^7 m^{-2}, respectively estimated using Eqs. (2) and (3).

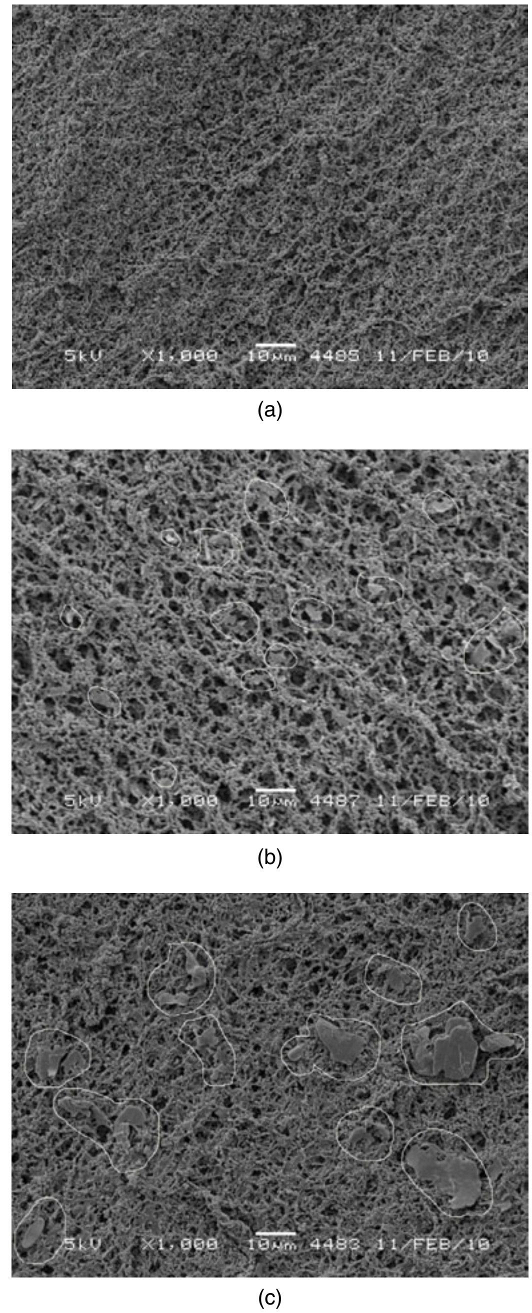

Fig. 15. (a) Virgin membrane M7. (b) Ultrapure water filtered through M7 using a graphite gear pump. (c) Ultrapure water filtered through M7 using a PTFE gear pump. Wear of the gear pump can be source for contamination by particles in the SDI setup.

4.5. Personal experience

Two non-experienced volunteers (persons A and B) were each asked to independently perform the SDI tests manually. The ASTM standard was handed out one week in advance to the volunteers. The SDI setup was assembled as shown in Fig. 2(b) and membranes M1 and

Table 7
SDI results obtained by two non-experienced volunteers and one with the automatic SDI setup

	SDI value	t_1(s)/t_2(s)	Normalized SDI for R_M (SDI+)
A	4.8	29.9/107.6	–
B	4.4	27/78	–
Automatic SDI setup	4.1	27.6/72.1	4.4

M7 were available for the test. Sufficient feed solution consisting of 4 mg l^{-1} of AKP-15 particles was prepared in a big tank for three SDI tests (person A, person B and an experienced test person using the automated SDI setup shown in Fig. 2(a)). The SDI results of persons A and B were compared to the SDI results obtained using the automated setup in Table 7.

4.5.1. Person A

Person A chose to do the SDI test using the membrane M1. He checked the pore size mentioned on the membrane batch by the manufacturer. Person A did not check the O-ring condition nor the membrane polymer material.

4.5.2. Person B

Person B was more precise in performing the SDI test. She checked the O-ring condition, membrane polymer material and the precision of the stopwatch. She repeated the test two times due to a damage visually observed on the membrane. She faced a difficulty in maintaining a constant and stable pressure of 207 kPa. She was worried about the setup contamination and cleaning.

4.5.3. Both persons A and B

- Had no doubt that the membranes properties met the ASTM requirements;
- Faced difficulties in using two stopwatches, opening the valves and maintaining the pressure at the same time;
- Were confused by the t_f starting point: was it $t = 0$ or $t = t_1$;
- Flushed the system before the SDI test;
- Chose a graduated cylinder;
- Monitored the temperature accurately throughout the test.

From Table 7 we can conclude that apparently different persons who got the same procedure and setup came to different SDI values as a result of differences in personal experience. Due to the fact that in the case of using the automated setup R_M was determined, the SDI could be normalized for the effect of the membrane resistance to SDI+. Moreover, the automated SDI setup is more accurate in measuring t_1 and t_2.

4.6. Commercial SDI devices

Several SDI devices are commercially available (Annex 1–5). The biggest advantage of the automated SDI devices is that the human error is less compared to manual devices. However, the SDI obtained from the commercial devices is not corrected for temperature, pressure and membrane properties. The commercial SDI devices do not consider the effect of the variation in the membrane properties. Most of the commercial SDI devices use a feed pump (or booster pump) which can be a source for additional particles. The feed pump requires time to maintain a constant and stable pressure in the beginning, which affects the final SDI result. The accuracy of the equipment and the SDI results are not mentioned in the instruction manuals of most devices.

Table 8
The effects of accuracy errors of the lab and field equipment on $SDI_O = 3$

Parameter	Lab		Field	
	Error±	Influence $SDI_O = 3\pm$	Error±	Influence $SDI_O = 3\pm$
T	1 [°C]	0.03	5 [°C]	0.15
dP	7 [kPa]	0.05	10 [kPa]	0.06
R_M	0.1×10^{10} [m^{-1}]	0.20	0.2×10^{10} [m^{-1}]	0.39
A_M[D = 47 mm]	2 [mm]	0.00	4 [mm]	0.00
t_1	1 [s]	0.03	5 [s]	0.17
t_2	1 [s]	0.07	5[s]	0.57
t_{15}	10[s]	0.02	15[s]	0.03
V_1	5 [ml/500 ml]	0.00	50 [ml/500 ml]	0.37
V_2	5 [ml/500 ml]	0.00	50 [ml/500 ml]	0.37
Total error		0.4		2.11

The pressure gauge and the flow meter need regular calibration which often is not done. The regular calibration is not mentioned in the manuals of the available commercial SDI devices.

4.7. Summary of the effects of accuracy errors on SDI = 3

Table 8 shows the effects of errors due to the accuracy of the equipment in the lab and the field at $SDI_O = 3$, assuming cake filtration, the reference testing conditions in Table 4, different equipment inaccuracies and the experienced errors.

5. Conclusions and recommendations

The SDI is sensitive for errors due to a low accuracy of equipment, different membrane properties, and variations in the testing parameters. Both mathematical models as well as experimental results show that a variation in the membrane resistance R_M has the highest impact on the SDI results. A 10% error in R_{MO} results in a ±0.25 variation for $SDI_O = 3$. The variation in R_M the ASTM standard allows is responsible for an SDI range of 2.29–3.98 at the level of SDI = 3. In addition, a 1 sec error in measuring the time to collect the second sample t_2 results in a variation ±0.07 at SDI = 3. Artifacts and personal experience also influence SDI results.

The total error in measuring the SDI can sum up to ±2.11 in the field and ±0.4 in the lab at the level of $SDI_O = 3$. This large error in the SDI values might have large consequences for pretreatment evaluation at desalination plants.

The following advices and recommendations are based on the theoretical results and personal experience. Besides the ASTM protocol, we believe that these recommendations are important for reliable and reproducible SDI result and should be mentioned in an updated version of the ASTM standard.

It is strongly recommended to use fresh SDI feed water. The SDI feed water should not be stored close to a heat source. The SDI setup should be cleaned and flushed well with clean water (RO production) before the test. After that, the SDI setup should be flushed with the SDI feed water to remove the residual clean water and guarantee a constant feed water quality from $t = 0$ on. The pressure gauge and the filter holder should be positioned at the same level. Accurate equipment is needed for reliable SDI results. The membrane should not be touched with the experimenter's hands; tweezers should be used. The support plate has to contain delicate bulges and have a low resistance. It is recommended to use an adjusted filter holder with a relief air valve. It is recommended to place filter paper under the membrane. t_0 for the test membrane should be between 25 and 50 s, where t_0 is the time to collect 500 ml of clean water under a pressure difference of 91.4–94.7 kPa. Preferably, new membranes should be used which should be stored in a dry and covered place. Last but not least, the SDI should be corrected for temperature, pressure and membrane resistance. For normalizing SDI for the testing conditions, available charts and tools can be used [35].

Acknowledgements

The authors of the paper would like to acknowledge the scientific and financial support of Vitens and Norit Process Technology B.V./X-Flow B.V. Part of this work is carried out in the framework of the InnoWATOR subsidy regulation of the Dutch Ministry of Economic Affairs (project IWA08006 "Zero Chemical UF/RO System for Desalination").

Symbols

A_M	—	membrane area (m^2)
A_{M0}	—	reference membrane area 13.4×10^{-4} (m^2)
C	—	scaling factor proportional to the foulants concentration
dP	—	applied pressure (Pa)
dP_o	—	reference applied pressure 207 (Pa)
I	—	fouling potential index (m^{-2})
J	—	flux ($m^3\ m^{-2}\ s^{-1}\ bar^{-1}$)
J_O	—	initial flux ($m^3\ m^{-2}\ s^{-1}\ bar^{-1}$)
m	—	fouling mechanism parameter (0, 1, 1.5 and 2)
MFI	—	modified fouling index ($s\ l^{-2}$)
n	—	number of data points
$\%P$	—	plugging ratio (%)
R_i	—	total resistance at data point i
R_C	—	specific cake resistance (m^{-2})
R_M	—	membrane resistance (m^{-1})
R_{Mo}	—	reference membrane resistance 1.29×10^{10} (m^{-1})
R_i	—	total resistance at data point i
SDI	—	silt density index (% min^{-1})
$t_{1,2}$	—	time to collect the first and second sample (s)
t_f	—	elapsed filtration time 15 (min) or 900 (s)
T	—	temperature (°C)
T_o	—	reference temperature 20°C
V	—	filtered volume (m^3)
$V_{1,2}$	—	sample volume (m^3)
$w_{R,A,V}$	—	fouling potential (m)
w	—	filtration state (m)
w_i	—	local accumulated filtrated volume at data point i

Greek

μ — viscosity (Pa s)

Annex 1

1. Field apparatus.
2. Filter holder, different sizes and material.
3. Filter holder, support plates.
4. Support plate, active area estimated using Image J software.
5. Automatic SDI device.

References

[1] V. Bonnelye, M.A. Sanz, J.-P. Durand, L. Plasse, F.d.r. Gueguen and P. Mazounie, Reverse osmosis on open intake seawater: pre-treatment strategy, Desalination, 167 (2004) 191–200.
[2] C.K. Teng, M.N.A. Hawlader and A. Malek, An experiment with different pretreatment methods, Desalination, 156 (2003) 51–58.
[3] D. Vial and G. Doussau, The use of microfiltration membranes for seawater pre-treatment prior to reverse osmosis membranes, Desalination, 153 (2002) 141–147.
[4] D. Vial, G. Doussaua and R. Galindob, Comparison of three pilot studies using Microza membranes for Mediterranean seawater pre-treatment, Desalination, 156 (2003) 43–50.
[5] S. Lueck, Reducing RO Operating Costs with Automated Monitoring Technology, in: International Water Conference, IWC, Pittsburgh, 1999.
[6] A. Nahrstedt and J. Camargo-Schmale, New insights into silt density index and modified fouling index measurements, in: IWA2008, San Francisco, CA, USA, 2008.
[7] Y. Zhao, J. Taylor and S. Hong, Combined influence of membrane surface properties and feed water qualities on RO/NF mass transfer, a pilot study, Water Res., 39 (2005) 1233–1244.
[8] E.M. Vrijenhoek, S. Hong and M. Elimelech, Influence of membrane surface properties on initial rate of colloidal fouling of reverse osmosis and nanofiltration membranes, J. Membr. Sci., 188 (2001) 115–128.
[9] M. Nystrom, A. Pihlajamiiki and N. Ehsani, Characterization of ultrafiltration membranes by simultaneous streaming potential and flux measurements, J. Membr. Sci., 87 (1994) 245–256.
[10] M. Elimelech and A.E. Childress, Zeta Potential of Reverse Osmosis Membranes: Implications for Membrane Performance, in: Water Treatment Technology Program Report No. 10, Department of Civil and Environmental Engineering/University of California, Los Angeles, CA, 1996.
[11] M. Elimelech, W.H. Chen and J.J. Waypa, Measuring the zeta (electrokinetic) potential of reverse osmosis membranes by a streaming potential analyzer, Desalination, 95 (1994) 269–286.
[12] M. Ernst, A. Bismarck, J. Springer and M. Jekel, Zeta-potential and rejection rates of a polyethersulfone nanofiltration membrane in single salt solutions, J. Membr. Sci., 165 (2000) 251–259.
[13] R. Ziel, A. Haus and A. Tulke, Quantification of the pore size distribution (porosity profiles) in microfiltration membranes by SEM, TEM and computer image analysis, J. Membr. Sci., 323 (2008) 241–246.
[14] M. Chandler and A. Zydney, Effects of membrane pore geometry on fouling behavior during yeast cell microfiltration, J. Membr. Sci., 285 (2006) 334–342.
[15] A. Alhadidi, A.J.B. Kemperman, J.C. Schippers, M. Wessling and W.G.J. van der Meer, The influence of membrane properties on the Silt Density Index, J. Membr. Sci., 383 (2011) 1–2.
[16] S.G. Yiantsios, D. Sioutopoulos and A.J. Karabelas, Colloidal fouling of RO membranes: an overview of key issues and efforts to develop improved prediction techniques, Desalination, 183 (2005) 257–272.
[17] M. Manttari, A. Pihajamaki and M. Nystrom, Effect of pH on hydrophilicity and charge and their effect on the filtration efficincy of NF membrane at different pH, J. Membr. Sci., 280 (2006) 311–320.
[18] S.G. Yiantsios and A.J. Karabelas, An assessment of the silt density index based on RO membrane colloidal fouling experiments with iron oxide particles, Desalination, 151 (2003) 229–238.
[19] J.C. Schippers and J. Verdouw, The modified fouling index, a method of determining the fouling characteristics of water, Desalination, 32 (1980) 137–148.
[20] J. Hermia, Constant pressure blocking filtration laws—application to power-low non-newtonian fluids, Trans. Inst. Chem. Eng., 60 (1982) 183–187.
[21] B. Blankert, B.H.L. Betlem and B. Roffel, Dynamic optimization of a dead-end filtration trajectory: blocking filtration laws, J. Membr. Sci., 285 (2006) 90–95.
[22] A. Alhadidi, B. Blankert, A.J.B. Kemperman, J.C. Schippers, M. Wessling and W.G.J. van der Meer, Effect of testing conditions and filtration mechanisms on SDI, J. Membr. Sci., 381 (2011) 142–151.
[23] F. Rossignol, A.L. Penard, F.H.S. Nagaraja, C. Pagnoux and T. Chartier, Dispersion of alpha-alumina ultrafine powders using 2-phosphonobutane-1,2,4-tricarboxylic acid for the implementation of a DCC process, J. Eur. Ceram. Soc., 25 (2005) 1109–1118.
[24] A. Alhadidi, A.J.B. Kemperman, J.C. Schippers, M. Wessling and W.G.J. van der Meer, Silt density index and modified fouling index relation, and effect of pressure, temperature and membrane resistance, Desalination, 273 (2011) 48–56.
[25] M. Elimelech, J. Gregory, X. Jia and R.A. Williams, Particle Deposition and Aggregation - Measurement, Modelling and Simulation, Elsevier, UK, 1995.
[26] V. Privman, H.L. Fr'isch, N. Ryde and E. Matijevic, Particle adhesion in model systems. Part 13: Theory of multilayer deposition, J. Chem. Soc. Faraday Trans., 87 (1991) 1371–1375.
[27] L. Song and M. Elimelech, Dynamics of colloid deposition in porous media: Modeling the role of retained particles, Colloids Surf. A, 73 (1993) 49–63.
[28] L. Song and M. Elimelech, Particle deposition onto a permeable surface in laminar flow, J. Colloid Interf. Sci., 173 (1995) 165–180.
[29] A. Mosset, V. Bonnelye, M. Petry and M.A. Sanz, The sensitivity of SDI analysis: from RO feed water to raw water, Desalination, 222 (2008) 17–23.
[30] C.R. Rao, H. Toutenburg, A. Fieger, C. Heumann, T. Nittner and S. Scheid, Linear models: least squares and alternatives, Springer, New York, 1999.
[31] J.H. Roorda and J.H.J.M. van der Graaf, New parameter for monitoring fouling during ultrafiltration of WWTP effluent, IWA Publishing, UK, 2001.
[32] P. van den Brink, A. Zwijnenburg, G. Smith, H. Temmink and M. van Loosdrecht, Effect of free calcium concentration and ionic strength on alginate fouling in cross-flow membrane filtration, J. Membr. Sci., 345 (2009) 207–216.
[33] ASTM Standard (D 4189 – 07): Standard Test Method for Silt Density Index (SDI) of Water, D19.08 on Membranes and Ion Exchange Materials, 2007.
[34] P. Dillon, P. Pavelic, G. Massmann, K. Barry and R. Correll, Enhancement of the membrane filtration index (MFI) method for determining the clogging potential of turbid urban stormwater and reclaimed water used for aquifer storage and recovery, Desalination, 140 (2001) 153–165.
[35] A. Alhadidi, A.J.B. Kemperman, J.C. Schippers, M. Wessling and W.G.J. van der Meer, SDI normalization and alternatives, Desalination, 279 (2011) 309–403.